Spherical Cap Bubbles in Low Density Liquids

by

W. G. Davenport, F. D. Richardson, and A. V. Bradshaw

Imperial College of Science and Technology, Prince Consort Road, London, S.W.7

(*Received 14 October 1966; in revised form 9 December 1966*)

Chemical Engineering Science, 1967, Vol. 22, page 1221–1235.

Abstract

Measurements have been made of the rising velocities and the shapes of spherical cap bubbles in a column 15 cm in diameter. The liquids used were water, aqueous solutions of polyvinyl alcohol (PVA) with viscosities up to 216 cP and ethyl alcohol; the gases were air, nitrogen and carbon dioxide. With carbon dioxide mass transfer coefficients were also obtained. Relationships between the measured quantities and the properties of the various liquids are considered. Liquid viscosities up to 50 cP have no effect on either the rising velocity or the shape of spherical cap bubbles. The addition of 0.5 % PVA to water results in a sharp drop in the mass transfer coefficient. Further additions cause it to increase and almost return to its original value.

Messungen der Aufstiegsgeschwindigkeit und der Form von runden Blasen in einer Säule von 150 mm innerem Durchmesser wurden durchgeführt. Die hierbei verwendeten Flüssigkeiten waren Wasser, wässerige Lösungen von Polyvinylalkohol (PVA) mit Viskositäten bis zu 216 cP und Äthylalkohol; die Gase waren Luft, Stickstoff und Kohlensäure. Bei Kohlensäure wurden auch Massenübertragungskoeffizienten ermittelt. Die Beziehungen zwischen den gemessenen Mengen und den Eigenschaften der diversen Flüssigkeiten wurden berücksichtigt. Viskositäten bis zu 50 cP wirken sich weder auf die Aufstiegsgeschwindigkeit noch auf die Form der Kugelblasen aus. Ein Zusatz von 0.5 % PVA zum Wasser ergibt scharfes Absinken des Massenübertragungskoeffizienten. Weitere Zusätze haben neuerliches Ansteigen bis nahezu auf den ursprünglichen Wert zur Folge.

1. INTRODUCTION

The Importance of interactions between gas bubbles and liquids in many industrial processes is well known. Nevertheless, until recently, most of the investigations have been confined to small bubbles, less than 1 cm^3. Moreover, the liquid phases studied have generally been water or dilute aqueous solutions with similar properties.

The investigation described in this paper was concentrated on the behaviour of large single bubbles of spherical cap shape rising in liquids of widely different properties. Since mass transfer between the bubble and the liquid may be influenced both by the rising velocity and the bubble shape, the initial part of the investigation was confined to these two factors. Subsequently, the mass transfer phenomena themselves were studied.

2. MATERIALS

Liquids employed in the investigation were tap water, distilled water, industrial ethyl alcohol and aqueous solutions of polyvinyl alcohol, made by the addition of "Alcotex 88-40" powder to warm distilled water. The properties of these liquids are given in Table 1, where the references indicate literature values. The properties of the polyvinyl alcohol solutions were measured by standard techniques apart from the carbon dioxide diffusion coefficients which were determined by the laminar film absorption method developed by Davidson and Cullen, [8].

Bubbles were formed from cylinder air, nitrogen and carbon dioxide, the last two having less than 50 parts per million residual impurities, apart from moisture.

Liquid	Density ($\mathrm{g\,cm^{-3}}$)	Surface Tension ($\mathrm{dyn\,cm^{-1}}$)	Viscosity (cP)	Solubility of $CO_2 \times 10^5$ ($\mathrm{mol\,cm^{-3}}$)	Diffusivity of $CO_2 \times 10^5$ ($\mathrm{cm^2\,s^{-1}}$)	
Tap water (16 °C)	1.00	73	1.11	4.39	1.37 (15 °C) [8]	
Distilled water (16 °C)	1.00	73	1.11	4.37±0.04†	1.35±0.1 (15 °C)†	
Ethyl alcohol (17 °C) (Industrial absolute)	0.79	22	1.25	12.6[17]	2.7 (16 °C) [18]	
Aqueous polyvinyl alcohol (15 °C)						
Percent PVA 0.5 %	1.0†	49.7 †	2†	4.37±0.04†		
2.85 %	1.0†	47.5 †	20† (12.5 °C)	4.15†	1.3† (11 °C)	0.15
3.9 %	1.0†	47.0 †	43†	4.10†	1.45† (15 °C)	
5.4 %	1.0†	46.9 †	115†	4.06†	1.4† (15 °C)	
6.1 %	1.0†	46.2 †	216† (17 °C)	4.04†	1.2† (15.5 °C)	

† This work

Table 1: Liquids employed during the investigation. (Except where stated, all properties from [13])

3. APPARATUS AND PROCEDURES

The bubbles were produced in 15 cm i.d. Perspex tubes of lengths up to 300 cm. Single bubbles were formed by the injection of gas into an inverted cup of spherical cap shape followed by manual rotation of the cup into the upright position. The larger bubbles showed a tendency to break up but, with care, this manual technique could be used to obtain perfect bubbles of volumes up to 50 cm^3.

Bubble volumes were determined by measuring the amounts of gas displaced from above the liquid column into a soap film meter, during the filling of the cup. Tests, in which the volume and pressure of the ingoing gas and the volume displaced above the column were measured, showed that the bubble volumes were obtained with a standard deviation of $\pm 0.02\,cm^3$. The mean bubble velocities were determined by means of two photoelectric cells placed against the column, at different levels. The cells actuated a stopwatch via a solenoid so that transit times could be measured to within 0.01 s.

The shapes of bubbles rising in a 15 cm square perspex tank were recorded photographically using an electronic flash, with a peak period of $\frac{1}{800}$ s. Measurements were taken from projections of the 35 mm negatives. Comparisons between the volumes calculated from the linear dimensions so obtained and those measured directly indicated that the linear dimensions were accurate to approximately ±4 %.

The rates of transfer of CO_2 between bubbles and various liquids were determined by measuring the changes in bubble volume which occurred during passage up the column. The experiments covered both absorption and desorption. In absorption studies a predetermined volume of CO_2 was injected into the inverted cup and the displaced volume was measured precisely. The bubble was then released and the time of rise and the bubble volume at the surface were measured. Prior to each experiment both the liquid column and the gas space above were purged with nitrogen to ensure the system was free from CO_2. In the desorption studies the column was saturated with CO_2 prior to each measurement by injecting a stream of small CO_2 bubbles (approx 2 mm dia.) at the bottom. Nitrogen was then injected into the cup as quickly as possible in order to minimize the pickup of CO_2 prior to the bubble release. The time of rise and the initial and final volumes were measured as for the absorption studies. Fortunately a sudden change in the rate of movement of the soap film in the flowmeter occurred when the bubble broke surface. This facilitated precise measurement of the CO_2 transferred and the volume of the emergent bubble was taken to be that given by the flowmeter reading just prior to the change in rate.

In the experiments using ethyl alcohol, all gases were saturated with alcohol vapour to reduce the effect of vapour transfer upon bubble volume.

4. RISING VELOCITY

4.1. Results

Results of the velocity measurements are shown in Figure 1 where the equivalent radius is the radius of a sphere with the same volume as the spherical cap bubble. Since the change in hydrostatic pressure during the rise causes the bubble to expand, the particular volume chosen for calculating the equivalent radius was the arithmetic mean of the top and bottom values.

The spread of results for the velocities of bubbles of identical size rising in water was found to be ±1 % of the mean value. Part of the deviation from the mean may be attributable to some bubbles not rising completely axially in the column.

As predicted by the expressions of Rippin, [16] and of Davies and Taylor, [10], there was no measurable effect of liquid density. Though the experiments described here only covered the range from $0.79\,\mathrm{g\,cm^{-3}}$ (ethyl alcohol) to $1\,\mathrm{g\,cm^{-3}}$ (water), in a further investigation Davenport et al., [6], using mercury have shown that even a density of $13.5\,\mathrm{g\,cm^{-3}}$ does not affect the rising velocity. The mean terminal velocity is unaffected by surface tension in the range of $22\,\mathrm{dyn\,cm^{-1}}$ (ethyl alcohol) to $73\,\mathrm{dyn\,cm^{-1}}$ (water). The further investigation by Davenport et al. referred to above showed that identical terminal velocities were obtained in mercury with a surface tension of $487\,\mathrm{dyn\,cm^{-1}}$.

The results also show that surface active agents, namely small amounts (0.5 %) of polyvinyl alcohol, have no influence on the rising velocity of the bubbles. This confirms the results of previous workers, [2, 11] and it would appear such substances only influence smaller bubbles.

Additions of PVA up to 4.5 %, which increase the viscosities of the aqueous solutions to 54 cP, have no appreciable effect on the rising velocity. Further additions to 115 cP cause some reduction in the velocity and this is even more marked when the viscosity is increased to 216 cP. This effect is especially noticeable with bubbles of an equivalent radius less than 1 cm. Since the PVA behaves like a Newtonian fluid, the effect of viscosity cannot be attributed to non-Newtonian behaviour. The column length showed no appreciable influence on mean velocity.

Velocity measurements on bubbles in water, which were either absorbing or desorbing CO_2 showed that the terminal velocity was not affected by mass transfer.

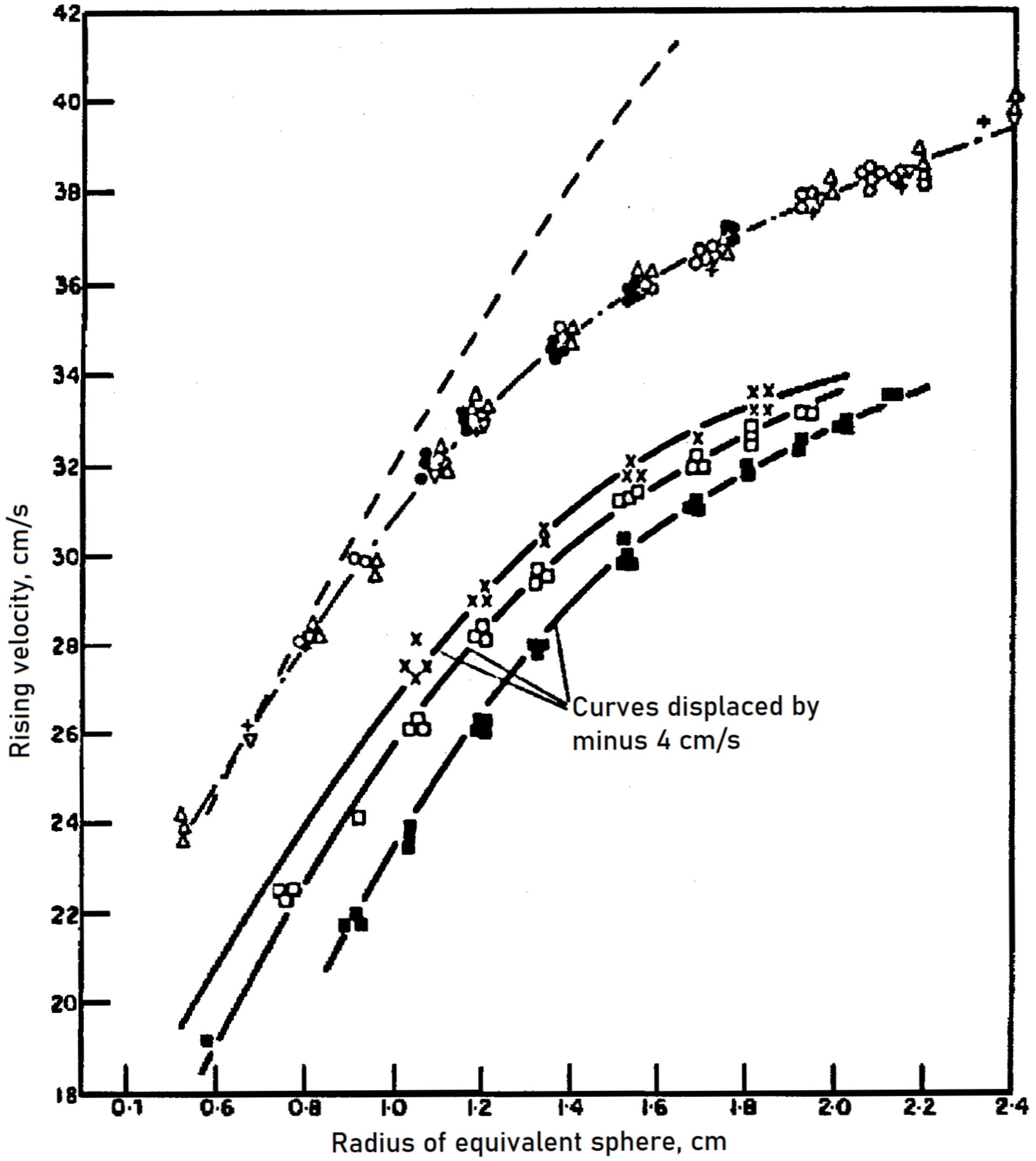

Figure 1: Bubble velocities vs. radius of equivalent sphere.
Air in water in 70 cm column +; air in water in 139 cm column ▽; air in water in 234 cm column △; nitrogen in ethyl alcohol 139 cm column ○: nitrogen in aqueous 0.5 % PVA solution 139 cm column ●.
- - - - Equation 6;– · – · – · – Equation 7 combined with Equation 6.
The following points and associated curves have been displaced by $-4\,\mathrm{cm\,s^{-1}}$.
Air bubbles rising in aqueous PVA solutions of various viscosities:
54 cP ×; 115 cP □; 216 cP ■

4.2. Discussion on rising velocities

A force balance on a single bubble rising in a fluid may be written as:

Net buoyancy force − Drag = Rate of change of bubble momentum.

The last term must include the virtual mass of the bubble to account for that part of the momentum stored in the flow pattern of the surrounding liquid. Since a bubble of gas rising in water reaches steady state conditions very rapidly (i.e. within about one bubble diameter), [15], it is satisfactory to simplify the above expression by neglecting the unsteady state term. This simplification is also adequate for the cases of mass transfer considered in this paper since the rate of change in momentum due to mass transfer is small compared with the actual momentum associated with the bubble. Therefore the above equation may be written as

$$F_d = \frac{4}{3}\pi r_e^3 \cdot (\rho_l - \rho_g) \cdot g\,. \tag{1}$$

If the coefficient of drag (C_d) is defined on the basis of the projected area of an equivalent spherical bubble, then

$$C_d = \frac{F_d}{\frac{1}{2}\rho_l U^2 \cdot (\pi r_e^2)} = \frac{8}{3} \cdot \frac{g r_e}{U^2} \cdot \left(1 - \frac{\rho_g}{\rho_l}\right) = \frac{4}{3\,\mathrm{Fr}}\,, \tag{2}$$

where Fr is a FROUDE number

$$\mathrm{Fr} \equiv \left[\frac{U^2}{2 \cdot \left(1 - \frac{\rho_g}{\rho_l}\right) \cdot g r_e} \right].$$

Since $\frac{\rho_g}{\rho_l} \ll 1$, it can usually be neglected in the above expression.
A dimensional analysis to find the dimensionless groups which may affect the velocity, providing the density and viscosity of the gas phase can be ignored, leads to a relationship between four such groups:

$$f\left(C_d, \mathfrak{R}, \mathrm{We}, \frac{r_e}{r_t}\right) = 0 \tag{3}$$

or

$$f\left(C_d, \mathrm{We}, \mathrm{Mo}, \frac{r_e}{r_t}\right) = 0\,, \tag{4}$$

where $\mathfrak{R}$ is the REYNOLDS number, $\mathfrak{R} = \frac{2\rho_l U r_e}{\mu}$, We is the WEBER number, $\mathrm{We} = \frac{2\rho_l U^2 r_e}{\gamma}$, and the parameter Mo represents the MORTON number, $\mathrm{Mo} = \frac{g\mu^4}{\rho_l \gamma^3}$.
As shown by HABERMANN and MORTON, [11], these groups are not sufficient to describe the behaviour of small bubbles completely. In the case of large

bubbles of spherical cap shape rising in liquids of low viscosity, the Reynolds, Weber and Morton numbers are not important. Form drag predominates and Davies and Taylor, [10], have shown experimentally that the velocity of these bubbles is given by

$$U = \frac{2}{3} \cdot \sqrt{g \cdot R_c}\,, \tag{5}$$

where R_c is the radius of curvature of the spherical cap. This velocity gives the correct pressure distribution in the immediate vicinity of the forward stagnation point, assuming that the flow in this region conforms to potential flow around a sphere. Habermann and Morton obtained an almost identical result but expressed the velocity in terms of an equivalent radius

$$U = 1.02 \cdot \sqrt{g \cdot r_e}\,. \tag{6}$$

While it is shown that the results reported here are in agreement with previous investigations on spherical cap bubbles, it will be seen from Figure 1 that the terminal velocity falls below that predicted by Equation 6. This discrepancy is attributable to wall effects since downward flow must occur between the bubble and the container walls. Uno and Kintner, [20], carried out a number of experiments to investigate wall effect and developed the following expression, which agrees satisfactorily with the results of this investigation

$$U_w = 1.09 \cdot U \cdot \left(1 - \frac{d_e}{d_t}\right)^{0.765} \tag{7}$$

where U_w is the velocity in the presence of the wall and U is the velocity in an infinite medium.

The retarding effect of viscosity above 54 cP is not clearly understood. It is unlikely to be due to the proximity of the bubble to the walls since the effect is less the larger the bubble. As indicated in Figure 2, if the velocity is plotted versus the square root of the observed radius of curvature, all the points lie on the same curve. Thus Equation 5 appears to hold even with these viscous liquids. Since the equation was derived on the assumption of inviscid flow, it is unlikely to apply under more extreme conditions. The shape of the bubble obviously alters as the viscosity changes from 100 cP to 200 cP, so that a relation which predicts velocities should take account of the viscosity of the fluid. Davidson has also observed a decreasing radius of curvature and reduced velocity of spherical cap bubbles in viscous media, [7]. He attributes these observations to viscous forces within the body of the fluid, which result from the distortions of the stream lines around the body. There are other factors which merit consideration. The decreased radii of curvature in viscous solutions are likely to reduce the coefficient of form drag even though the overall coefficient of drag has obviously increased. The coefficient of skin friction drag may have increased due to the presence of surface active agents accumulating towards the rear of the bubble and producing an immobile interface.

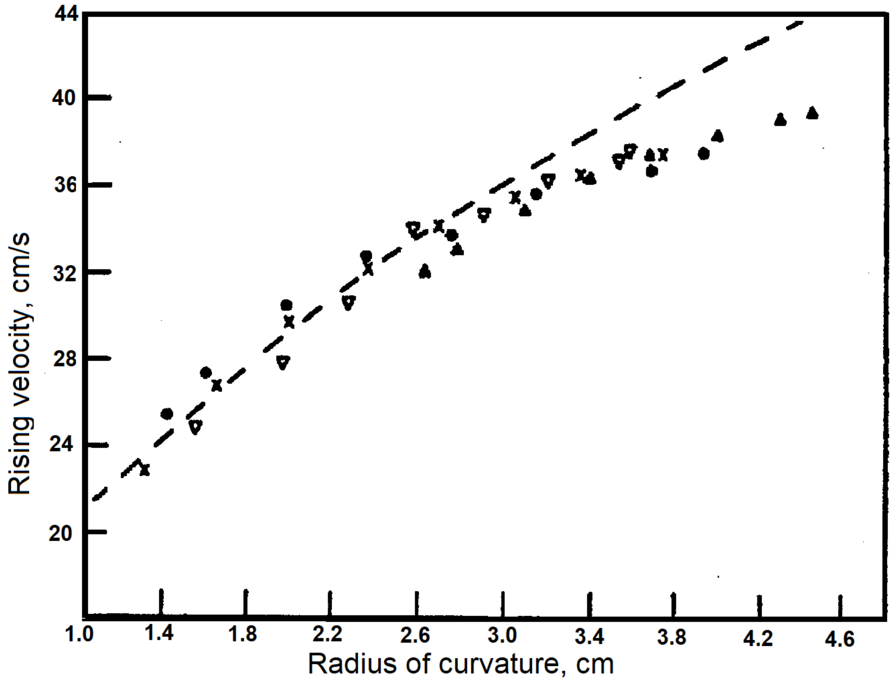

Figure 2: Velocities of bubbles as a function of radius of curvature.
water ▲; 54 cP ▽; 115 cP ×; 216 cP ●. broken line Equation 5

The increased viscosity reduces the Reynolds number. For example, the Reynolds number based on the equivalent diameter[1] for a 2 cm diameter bubble rising in water is 6×10^3. The corresponding values for the same size of bubble in 5.4 % and 6.1 % PVA solutions are 50 and 25 respectively. From the results of Habermann and Morton, [11], the drag coefficient and the bubble shape appear markedly dependent on the Reynolds number when this is below 2×10^3 and moreover, the Weber or the Morton number is often an important additional parameter. This implies that in general both bubble shape and rising velocity are dependent on an interaction of hydrodynamics, surface tension and viscous forces. In the case of large bubbles in viscous solutions, surface tension forces are likely to be relatively small and hence it is not surprising that the viscosity influences the terminal velocity even though the bubble shape remains spherical cap.

---

[1] The Reynolds numbers based on the basal diameter are 11.5×10^3, 95 and 36 for water for 5.4 % PVA solution and for 6.1 % PVA solution respectively.

5. BUBBLE SHAPE

5.1. Results

The observed shapes and characteristics of bubbles rising in liquids are outlined in Table 2. The measured heights and basal radii for bubbles rising in water and PVA solutions are shown in Figure 3. The large bubbles were of the spherical cap shape observed by previous investigators, [10, 11]. Photographs showed that the curvature of the front surface of bubbles greater than 10 cm^3 was very nearly spherical. On any particular bubble the distance from the front surface to the centre of curvature was within ±4 % of the mean radius.

In low viscosity liquids the rear surface showed pronounced rippling but, with increasing PVA, these ripples were damped out. In solutions containing not less than 4.5 % PVA, corresponding to viscosities greater than 54 cP, the rear surface became slightly concave. This could be due to a stagnation point produced by a trailing annular vortex. The maximum penetration at this point is 3 mm, which corresponds to an upward velocity relative to the bubble of some 20 cm s^{-1} to 24 cm s^{-1}, which is similar to velocities in the trailing vortex which were observed visually.

Large bubbles, greater than 15 cm^3, rising in 6.1 % PVA solution with a viscosity of 216 cP, developed long, thin peripheral skirts as sketched in Figure 4. Measurements of the dimensions of the main body of the bubble indicated that only small amounts of gas were present in these skirts. The development of such skirts has not previously been reported. However, recent photographs of large bubbles rising in glycerine and oil, [1], suggest the presence of a trailing gas envelope.

5.2. Discussion on bubble shape

Dimensional analysis can also be used to relate bubble shape to other liquid properties. If the gas properties are not important and the only relevant liquid properties are density, viscosity and surface tension, the shape, which for a spherical cap bubble may conveniently be expressed in terms of a width to height ratio E, equal to $\frac{2a}{b}$, [15], will be related to the other properties by

$$f\left(E, \mathfrak{R}, \mathrm{Mo}, \frac{r_e}{r_t}\right) = 0 \tag{8}$$

Since neither the surface tension nor the viscosity are likely to be important in the case of large bubbles, E should be constant for low values of $\frac{r_e}{r_t}$. However, even though the results of the present tests show less scatter than those of Davies and Taylor, [10], (Figure 3), there is still some doubt about the constancy of the value of E, which for an equivalent radius of less than 1 cm appears to be influenced by liquid properties.

With larger bubbles, equivalent radius 2 cm, the ratio of width to height decreases with size as would be expected if the proximity of the walls were

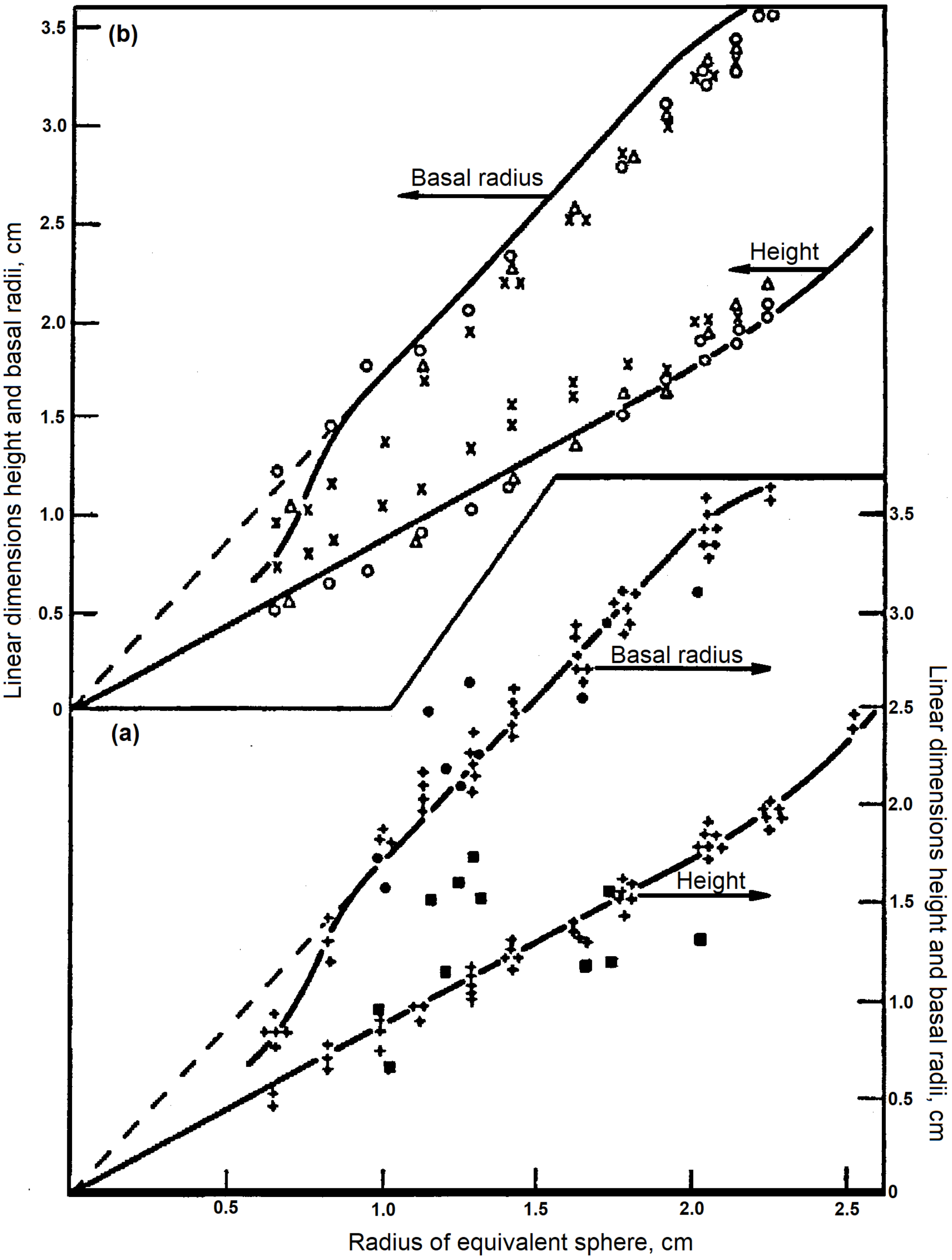

Figure 3: Heights and basal radii for rising bubbles as a function of equivalent radius.
Lower graph (a) bubbles in water +; Davies and Taylor results [10] height ■, basal radius ●.
Upper graph (b) bubbles in PVA solutions; 54 cP ○, 216 cP ×; lines as for water.

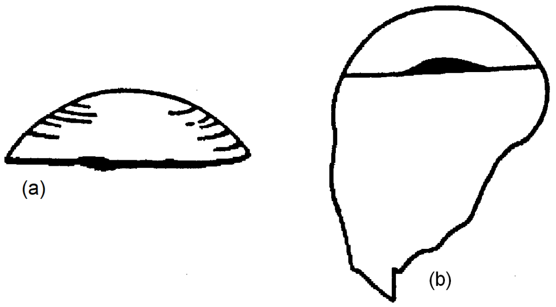

Figure 4: Sketches showing relative shapes of 20 cm^3 bubbles in (a) water and (b) 216 cP PVA solution

influencing bubble shape. Figure 3 also indicates that as the concentration of PVA increases and the solutions become more viscous, the ratio of the width to the height again decreases. This effect, which implies a decreasing radius of curvature with increasing PVA, is most noticeable with smaller bubbles ($r_e \approx 1.7$) in the 216 cP solution. In addition, as Table 2 shows, the size at which the spherical cap shape is adopted appears to decrease as the viscosity increases.

Liquid	Bubble volume, cm^3	r_e	Remarks
Tap water and distilled water	0.04–4.5	0.21–1.02	Ellipsoidal bubbles—marked oscillation. Helical rise. Transition to spherical cap at $4.5\,\text{cm}^3$. The transition from spherical cap to ellipsoidal is very noticeable during absorption of CO_2 from bubbles of suitable size range.
	4.5–40	1.02–2.1	Spherical cap bubbles. Rippling evident both on rear and front surfaces and on the relatively plane undersurface.
Ethyl Alcohol	< 1	< 0.62	Ellipsoidal bubbles with marked oscillation.
	1–40	0.62–0.95	Spherical cap bubbles as for water. Rippling slightly more pronounced.
0.5 % PVA ($\mu = 2\,\text{cP}$)	< 1	< 0.62	Ellipsoidal bubbles with no oscillation.
	1–3.5	0.62–0.95	Ellipsoidal bubbles. Oscillations evident but less noticeable than with ethyl alcohol or water.
	3.5–40	0.95–2.1	Spherical cap bubbles-rectilinear rise. Rippling much less pronounced than with water.
4.2 % PVA ($\mu = 54\,\text{cP}$)	< 1	< 0.62	Ellipsoidal – no oscillation.
	1–3	0.62–0.89	Transition region. Ellipsoidal with slight oscillation.
	3–40	0.89–2.1	Spherical cap bubble. Rectilinear motion. Apart from initial release rippling very slight. Lower surface slightly concave.
5.4 % PVA ($\mu = 115\,\text{cP}$)	< 1	< 0.62	Ellipsoidal. No surface instability.
	1–1.5	0.62–0.71	Slight surface instability. Gradual change of shape to spherical cap.
	1.5–40	0.71–2.1	Spherical cap. Rectilinear rise. No rippling. Lower surface concave.
6.1 % PVA ($\mu = 2.6\,\text{cP}$)	0.2–15	0.36–1.5	Spherical cap. Rectilinear rise. No rippling or oscillation. No shape transition in this range.
	15–40	1.5–2.1	Bubble tends to form thin skirts of trailing gas. Length of skirt increasing with bubble size, up to approx. 30 cm long,

Table 2: General description

6. MASS TRANSFER

6.1. Results

The experimentally determined rates of absorption have been interpreted in terms of a mass transfer coefficient, β, defined as follows[2],

$$\dot{n} = -\beta A_l \cdot (C_l - C_b)\ . \tag{9}$$

A has been taken as the surface area of a spherical bubble with the same volume as the real bubble and is equal to $\left(36\pi V^2\right)^{\frac{1}{3}}$. Since the gas contained only CO_2, all the resistance to transfer was confined to the liquid. Baird and Davidson, [2], have shown that, under isothermal conditions and with equilibrium at the interface, the rate of mass transfer may be given by the following equation,

$$\dot{n} = \frac{1}{\mathscr{R}\theta} \cdot \left(P_B \cdot \frac{\mathrm{d}V}{\mathrm{d}t} + V \cdot \frac{\mathrm{d}P_B}{\mathrm{d}t}\right) = -\beta S V^{\frac{3}{2}} \cdot \left(P_{\mathrm{CO_2}} \cdot H - C_b\right) \tag{10}$$

where S is the shape factor, in this case $(36\pi)^{\frac{1}{3}}$ and H is the Henry's law constant. In the case of absorption from CO_2 bubbles into water free from CO_2,

$$P_{\mathrm{CO_2}} = P_B\ , \qquad C_b = 0\ . \tag{11}$$

Furthermore, since the velocity is only slightly dependent on the bubble volume, it has been assumed constant at a mean value $\overline{U}$. Hence

$$\frac{\mathrm{d}P_B}{\mathrm{d}t} = -\rho_l g \overline{U}\ . \tag{12}$$

Substitution in Equation 10 and integration with β constant leads to the following equation for the mass transfer coefficient in terms of other bubble parameters,

$$\sqrt{P_B^0 \cdot V^0} - \sqrt{P_B^T \cdot V^T} = \frac{1}{4} \cdot \frac{hSH\mathscr{R}\theta}{\rho_l g \overline{U}} \cdot \left(\sqrt[3]{(P_B^0)^4} - \sqrt[3]{(P_B^T)^4}\right)\ , \tag{13}$$

---

[2] This mass transfer coefficient may be related to the coefficient $h_l^\star$ used by Calderbank and Lochiel, [3], by,

$$\beta = h_l^\star \cdot \frac{A_T}{A}\ ,$$

where A_T is the total surface area of the bubble. The value of $\frac{A_T}{A}$ may be calculated from the ratio $\frac{2a}{b}$. From Figure 3(a), for bubbles between 1 cm and 2 cm equivalent radius rising in water, this ratio may be shown to equal 3.90, which gives $h_l^\star = 0.61 \cdot \beta$. For bubbles of the same size rising in 216 cP solution, the ratio $\frac{2a}{b}$ is 3.25 corresponding to a value of $h_l^\star = 0.68 \cdot \beta$. In spherical cap bubbles, with which this work is principally concerned, it is difficult to make a precise estimate of the proportion of mass transfer through the rear surface and consequently, it is not possible to separate completely the effect of changes in area from changes in mass transfer coefficient, which is the main reason for using $h_l^\star$. In addition, many of the bubbles exhibited a rippling surface which would make accurate estimation of the true area difficult. For this reason, the more common practice of using a coefficient based on the equivalent spherical area is preferred.

where the superscripts 0 and T refer to bubble properties at the time of release and at the top of the column respectively.
In the case of desorption, Equation 9 is still applicable and Equation 10 will also be valid if any transfer resistance in the gas phase is negligible compared with that in the liquid. However, Equation 11 no longer holds and the pressure of CO_2 in the bubble is given by

$$P_{\mathrm{CO}_2} = \left(n - n^0\right) \cdot \frac{\mathscr{R}\,\theta}{V} = \left(P_B - \frac{P_B^0 \cdot V^0}{V}\right) . \tag{14}$$

For desorption, the liquid in the column was saturated by small bubbles of CO_2 rising from the bottom. This could have resulted in a gradient of CO_2 concentration along the column, of at most 20 %, if no mixing had occurred during saturation or during each bubble experiment. Thus C_b could have varied with height according to the equation

$$C_b = P_{hs} \cdot H = P_B \cdot H \,, \tag{15}$$

and it is probably best to allow for this maximum variation. Substituting Equation 14 and Equation 15 into Equation 10 and integrating leads to

$$\sqrt[3]{\left(P_B^T \cdot V^T\right)^4} - \sqrt[3]{\left(P_B^0 \cdot V^0\right)^4} = \frac{\beta S H \mathscr{R}\,\theta}{\rho_l g \overline{U}} \cdot \left(P_B^0 \cdot V^0\right) \cdot \left(\sqrt[3]{(P_B^0)^4} - \sqrt[3]{(P_B^T)^4}\right) \tag{16}$$

No allowance has been made in any of the calculations for the transfer of water vapour or nitrogen between the liquids and the bubbles. Approximate calculations show that these effects should be much less than the experimental errors arising from the measurement of velocities and volumes. It is believed that the derived mass transfer coefficients are accurate to about ±20 %.
The mass transfer coefficients vs. the equivalent radius are shown in Figure 5 and Figure 6. This radius is based on the arithmetic mean of the bubble volume at release and at the top of the column. Since the volume changes were relatively small and, as may be seen from the graphs, β is not strongly dependent on r_c, the use of the arithmetic average volume will be within the limits of experimental accuracy. It is possible that unsteady conditions at and immediately following bubble release may have influenced the results and have caused the mass transfer coefficients recorded in experiments with the 164 cm column to be slightly higher than those from the 250 cm column (Figure 6). In view, however, of the comparatively good agreement with other investigators and the short duration of unsteady conditions, [15], such effects are not thought to be significant.

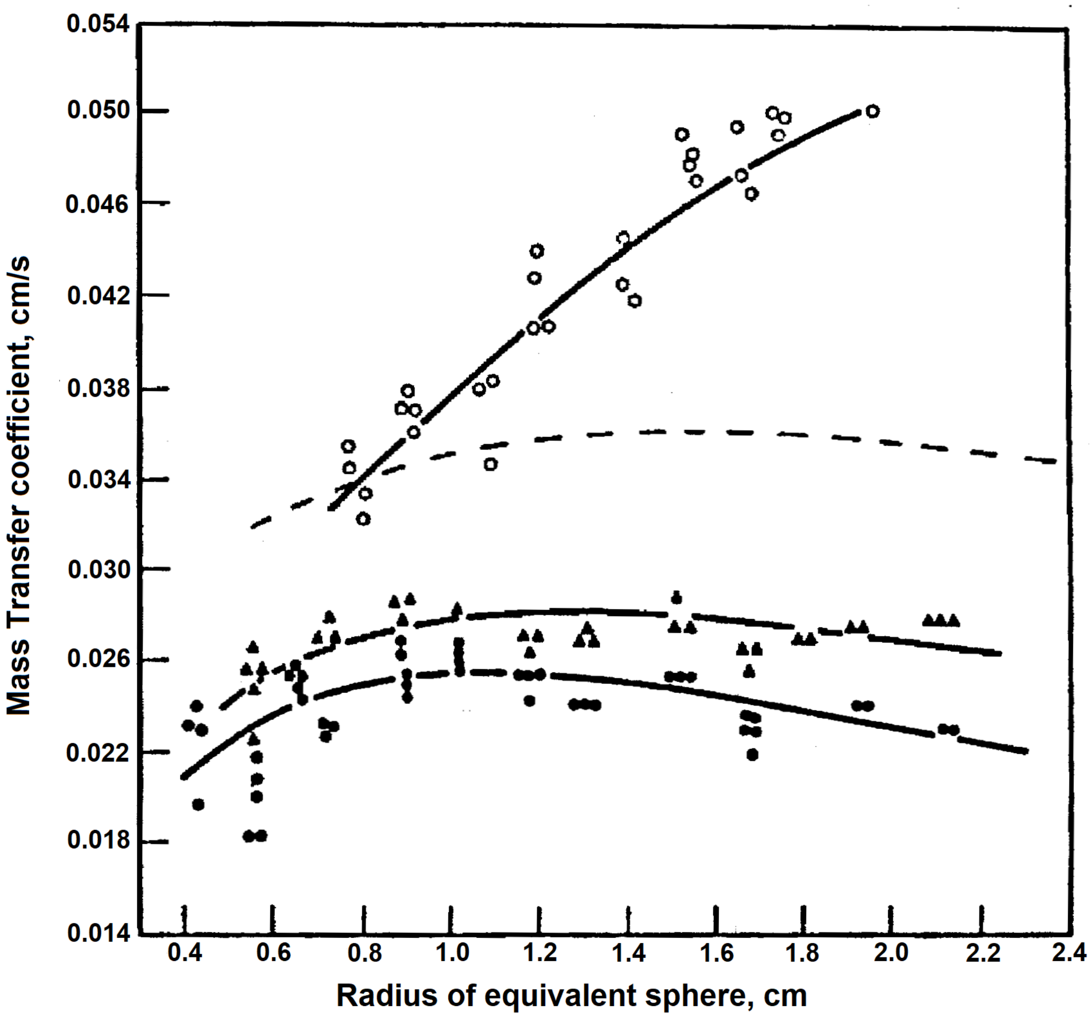

Figure 5: Mass transfer coefficient for CO_2 absorption in water and alcohol in 164 cm column: distilled water 19 °C ▲; tap water 16 °C ●; ethyl alcohol ○. Calculated curve for alcohol based on experimental results for water assuming $h_l \propto \sqrt{\mathscr{D}}$, broken line

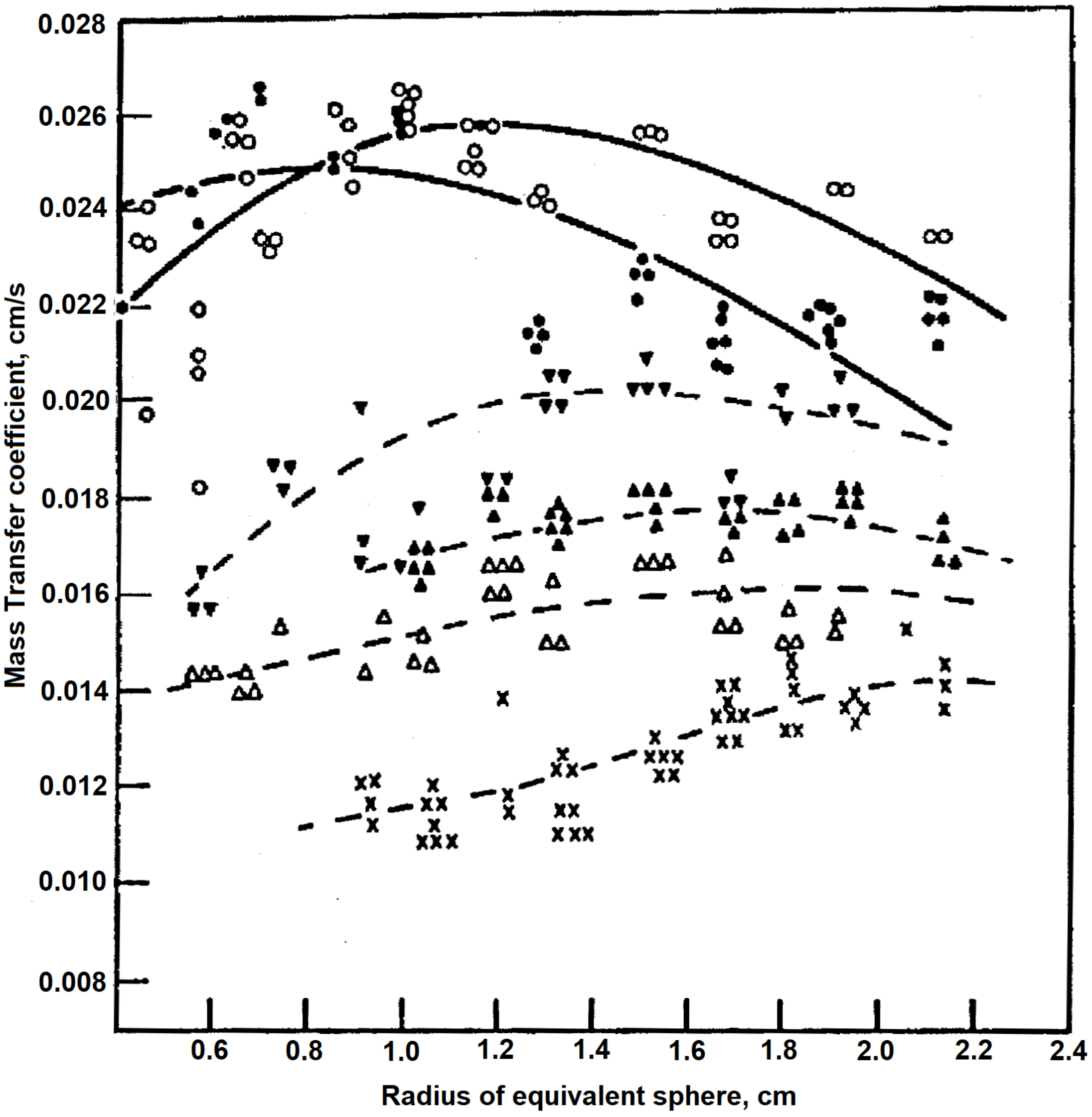

Figure 6: Mass transfer coefficients for CO_2 being absorbed by various liquids. Full lines: tap water absorbing; 164 cm column, 16 °C ○; 250 cm column, 15 °C ●. Broken lines: PVA solutions absorbing; 2 cP ×; 44 cP △; 58 cP ▲; 115 cP ▼

7. DISCUSSION OF RESULTS

7.1. Comparison with previous work

The majority of the earlier investigations have been confined to smaller bubbles. However, experiments by Leonard and Houghton, [14], and Baird and Davidson, [2], which have been shown in Figure 7, are in fair agreement with the present results where the ranges overlap. With the exception of results for a bubble of 1.25 cm equivalent radius, Calderbank and Lochiel's results[3] are higher than those obtained in the present investigation. This could be at least partially attributable to their use of purer solution. Their experiments were confined to a 4 in i.d. column; only specially purified distilled water was used and it was frequently changed. As shown later, surface active agents may considerably retard mass transfer even to large bubbles.

7.2. Absorption and desorption

In addition to the results in Figure 5 and Figure 6, the mean mass transfer coefficients obtained from measurements on CO_2 desorbing into nitrogen bubbles confirm the results from absorption and indicate that any resistance on the gas side of the interface is much less than on the liquid side. The desorption results were, however, less reproducible than the absorption experiments and this may be attributed to two causes. Firstly, some mass transfer occurs to the bubble while it is still in the cup so that the actual concentration difference is slightly less than the one used in the calculations. Secondly, a certain amount of mixing will be brought about by the bubble and some of the liquid in the bottom of the column will be carried up in the bubble wake. This will result in a concentration difference $(C_b - C_l)$ in this area, which is greater than the estimated one. Though these two errors act in opposite directions and may cancel out, they reasonably explain the scatter in the results. Another error may result from relating the CO_2 concentration in the liquid to the hydrostatic head (Equation 15) and neglecting the mixing effect of convection currents.

---

[3] These have been recalculated to give a mass transfer coefficient based on the area of the equivalent sphere.

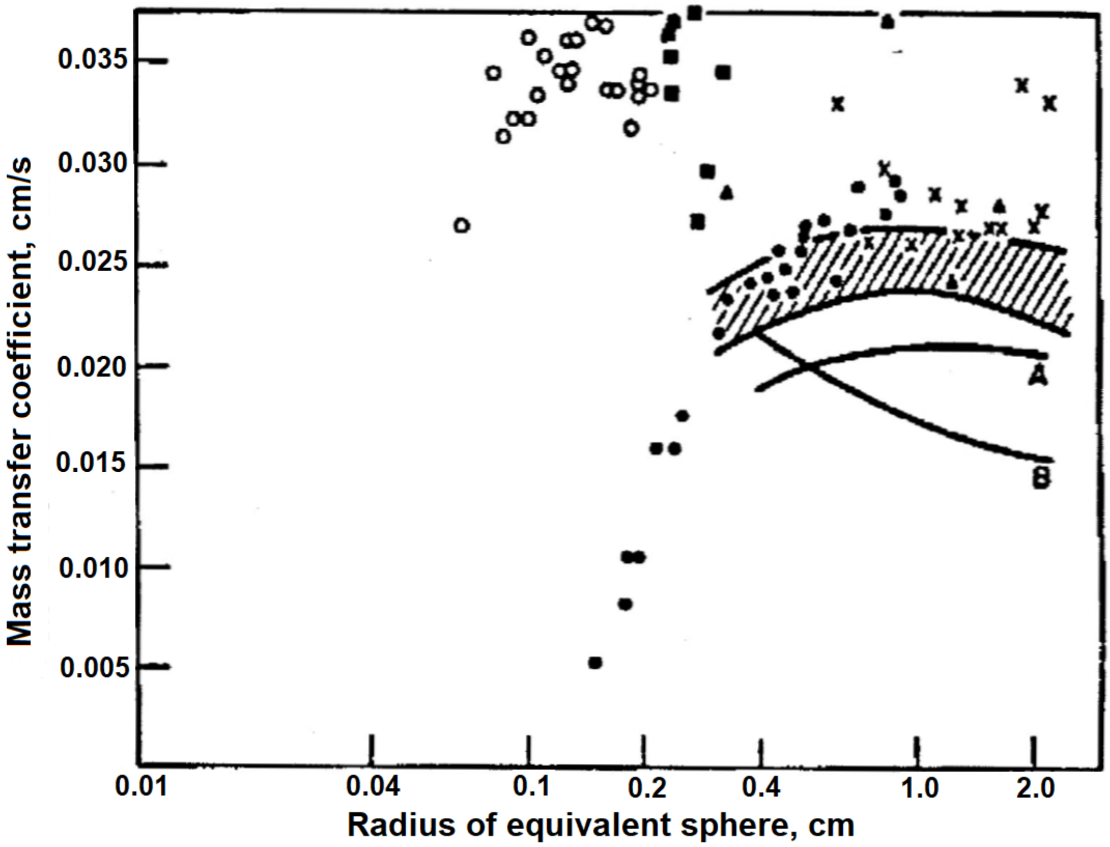

Figure 7: Comparison of mass transfer coefficients (related to the area of the equivalent spherical bubble) for CO_2 being absorbed by water, calculated from the results of various investigations:
this work shaded band; Baird and Davidson [2] ×; Leonard and Houghton [14] ●; Calderbank and Lochiel [3] ▲, each point representing a group of results which are close to one another; Coppock and Meiklejohn [4] ■; Hammerton and Garner for the absorption of ethylene into water [12] ○; Full lines A and B see text

7.3. The effect of surface active agents and viscosity

Because PVA reduces the surface tension of water, it is not possible to separate completely the effects of viscosity and surface activity. Trace amounts of surface active materials present in tap water are presumably responsible for the reduction of the mass transfer coefficient below that for distilled water shown in Figure 5. Figure 6 indicates that small additions of PVA to distilled water reduce the mass transfer coefficient by approximately 50 %, although the viscosity is only raised to 2 cP. Further additions of PVA cause a continuous increase in the mass transfer coefficient until 216 cP is reached. The curve for this viscosity (which is not shown in Figure 6) fell slightly below that for the 115 cP solution for bubbles up to 1.3 cm equivalent radius. Between 1.3 cm and 1.8 cm radius the mass transfer coefficients rose from 0.020 cm s^{-1} to 0.027 cm s^{-1}; they then fell to 0.026 cm s^{-1} for bubbles up to 2.1 cm radius.

The higher figures obtained in the 216 cP solution, for bubbles of 1.8 cm and above are almost certainly attributable to the additional surface area caused by the formation of skirts (see Table 2).

It is difficult to account for the effect of PVA concentration on mass transfer coefficient. One or more of the following factors may be important.

1. Small quantities of PVA reduce rippling and this in turn reduces the mass transfer rate. A similar effect was observed by Baird and Davidson, [2], using other surface active agents. However, this suppression of rippling fails to explain the increase of the mass transfer coefficients as the PVA concentration increases above 0.5 % for, with these solutions, rippling was damped even more effectively.

2. The presence of an additional film resistance due to an accumulation of surface active agents at the interface. This latter effect has been noted previously for ripple-free flow around a solid object, [5]. However, in the present series of experiments, the diffusion coefficients for CO_2 in the PVA solutions were measured using the spherical film absorption technique, [8]. In this method, solutions are passed over a spherical surface and the rate of absorption of CO_2 is measured. The diffusion coefficient is calculated on the basis of unsteady diffusion into an infinite liquid. The time for diffusion, which is that required for the fluid flow round the sphere, allows ample opportunity for surface active agents to concentrate at the gas-liquid interface. Their presence would be detected by a lowering of the apparent diffusion coefficient of CO_2. Since no such lowering was observed, as may be seen from Table 1, the presence of a film resistance to mass transfer is unlikely. However, measurements of the CO_2 diffusivity were not carried out at the concentrations of PVA (0.5 % to 1 %), which showed the maximum reduction in the mass transfer coefficient.

3. The formation of an immobile surface film due to the accumulation of surface active agents. Such a film would cause an appreciable velocity

gradient in the liquid at the bubble surface and thus cause a reduced rate of transfer compared with that obtained when potential flow occurs around the front section. A surface film may only require the presence of a limited concentration of surface active agents, sufficient to form a monolayer. Normally the presence of larger amounts would probably have no additional effect. When, however, as in the case of PVA, increased quantities of surface active agents raised the viscosity, the shear forces on the bubble surface would also increase. These forces would tend to remove the immobile surface film and to restore relative movement between the gas and the liquid, at least over part of the frontal surface of the bubble.

7.4. Theoretical models

Theoretical models for mass transfer into spherical cap bubbles have been proposed by BAIRD and DAVIDSON, [2], and by CALDERBANK and LOCHIEL, [3]. Both are based on unsteady state diffusion into the liquid flowing past the bubble. BAIRD and DAVIDSON relate their mass transfer coefficients to an area of equivalent volume sphere (as in this paper), whereas CALDERBANK and LOCHIEL relate theirs to the frontal area of the bubble.

SZEKELY, [19], has measured absorption of the CO_2 from the rear of a bubble held in a thin perspex dome. He reports that the rate of transfer per unit area through the rear surface is $\frac{1}{3}$ ($\pm 60\,\%$) that through the front. As the ratio of the frontal surface area to the rear is approximately $\frac{5}{4}$ (subtended half-angle 54°), it is evident that the transfer through the rear part of the bubble amounts to about 20 % of the total. When this amount of transfer is deducted from the results obtained with distilled water, the mass transfer coefficients represented by line A in Figure 7 are obtained. These may be compared with the values predicted Equation 17 for frontal transfer by the equation of BAIRD and DAVIDSON, represented by line B in Figure 7.

$$\beta = 0.975 \cdot d_e^{-\frac{1}{4}} \cdot \mathscr{D}^{\frac{1}{2}} \cdot g^{\frac{1}{4}} \,. \tag{17}$$

If the approach of LOCHIEL and CALDERBANK, [15], were adopted, Equation 17 would be replaced by

$$\beta = 1.13 \cdot d_e^{-\frac{1}{2}} \cdot \mathscr{D}^{\frac{1}{2}} \cdot U_w^{\frac{1}{2}} \,.$$

The use of this would reduce the values for the calculated mass transfer coefficients by approximately 3 % and 9 % for bubbles with r_e equal to 1 cm and 2 cm respectively, rising in a 15 cm dia. column.

The measured values lie somewhat above the calculated values: the difference may well be caused by ripples in the bubble surfaces which would enhance the rates of mass transfer.

The DAVIDSON and HARRISON model, [9], for mass transfer round spherical surfaces can be extended to account for mass transfer to a trailing skirt of gas, for the case where this has the shape of a cylinder extending vertically downwards from the base of the bubble. The rate of mass transfer through the skirt, $\dot{n}_{\text{skirt}}$, and the concentration, C, are given by

$$\dot{n}_{\text{skirt}} = 2\pi\,\mathscr{D} \cdot \int_{\Phi_1}^{\Phi_2} \left(\frac{\mathrm{d}C}{\mathrm{d}\Psi}\right)_{\Psi=0} \mathrm{d}\Phi \tag{18}$$

and

$$\frac{C - C_b}{C_i - C_b} = 1 - \frac{2}{\sqrt{\pi}} \cdot \int_0^{\frac{\Psi}{2\sqrt{\mathscr{D}\,\Phi}}} e^{-\eta^2}\,\mathrm{d}\eta\,. \tag{19}$$

In the region of the skirt, Ψ and Φ are defined as follows:

$$\begin{aligned} 2\pi \cdot \Psi &= 2\pi R_c \cdot \sin(\alpha) \cdot U_z \cdot y \\ \frac{\mathrm{d}\Phi}{\mathrm{d}z} &= R_c^2 \cdot \sin^2(\alpha) \cdot U_z \\ \Phi_2 &= R_c^2 \cdot \sin^2(\alpha) \cdot U_z \cdot l + \Phi_1\,. \end{aligned}$$

l is the length of the skirt and Φ_1 has the same value as given by DAVIDSON and HARRISON's equation, C.10, [9]. However, the definition of $\frac{\mathrm{d}\Phi}{\mathrm{d}z}$ is slightly different from that used by DAVIDSON and HARRISON, [9], because in the region of the skirt the stream lines are assumed to be parallel to the vertical axis. The slight change in the flow direction resulting from the approximation of the skirt to a vertical cylinder has been assumed to have a negligible effect on the concentration gradient. The surface velocity U_z has been taken as constant over the length of the skirt and equal to $\sqrt{2gb}$ or $\left[2gR_c \cdot \sqrt{1 - \cos(\alpha)}\right]$ where b represents the height of the bubble.[4] With these modifications the overall mass transfer rate becomes

$$\dot{n} = -4 \cdot \sqrt{\pi \cdot \mathscr{D} \cdot \Phi_2} \cdot (C_l - C_b)\,. \tag{20}$$

The quantity of gas in the skirt is small and may be neglected when relating the radius of curvature of the spherical cap and the subtended half-angle to the bubble volume or equivalent diameter. On this basis, Equation 20 can still be evaluated for the case of bubbles with skirts, to give the mass transfer coefficient based on the area of the equivalent sphere as

$$\beta = K \cdot d_e^{-\frac{1}{4}} \cdot \sqrt{\mathscr{D}} \cdot g^{\frac{1}{4}} \tag{21}$$

where

$$K = 1.78 \cdot \left[\frac{\sqrt{ms} \cdot \left(\frac{l}{R_c}\right) + 1.507 - 0.2667 \cdot s^{\frac{3}{2}} - 0.6667 \cdot ms^{\frac{3}{2}}}{(m^2 \cdot q)^{\frac{1}{4}}}\right]^{\frac{1}{4}} \tag{22}$$

---

[4] For bubbles subtending a 50° half-angle, the surface Velocity calculated from $\left[2gR_c \cdot \sqrt{1 - \cos(\alpha)}\right]$ is $0.84 \cdot \sqrt{gR_c}$. However, in the case of long skirts, this value will be an overestimate as the surface velocity must approach the terminal velocity given by Equation 5, ignoring wall effects. Since the mass transfer rate depends on the square root of the surface velocity, the estimate for the mass transfer coefficient over the skirt will not be more than 10 % too high.

and

$$\begin{aligned} m &= 1 - \cos(\alpha) \\ s &= 1 + \cos(\alpha) \\ q &= 2 + \cos(\alpha) \end{aligned}$$

and α is the half angle subtended by the bubble at the centre of curvature. For the 50° subtended half-angle found with water, the coefficient is given by

$$K = \sqrt{4.0 \cdot \left(\frac{l}{R_c}\right) + 0.95} \tag{23}$$

For a 65° subtended half-angle, which is applicable to bubbles in the more viscous solutions, the coefficient becomes

$$K = \sqrt{2.6 \cdot \left(\frac{l}{R_c}\right) + 0.87} \tag{24}$$

Measurements of skirt lengths in the 216 cP solution gave values for $\frac{l}{R_c}$ of about 1.4 for 20 mL bubbles and 1.8 for 30 mL bubbles. For a subtended half-angle of 65°, the mass transfer coefficients for such bubbles should be 2 to 2.5 times those for bubbles without skirts. This calculation neglects mass transfer from the inside surface of the skirt which would further increase this figure.

Experimental measurements showed that mass transfer coefficients for bubbles with skirts were only about 1.3 times those without. These provide further evidence that mass transfer at the interface is retarded by a film which either offers physical resistance to mass transfer or changes the hydrodynamic pattern so as to produce low velocities at the gas-liquid interface.

7.5. The effect of solute diffusivity

The models of HIGBIE, DANCKWERTS, BAIRD and DAVIDSON and CALDERBANK and LOCHIEL all indicate the mass transfer coefficient to be proportional to the square root of the diffusivity. The results of HAMMERTON and GARNER for small bubbles of hydrogen ($d_e = 0.7\,\mathrm{cm}$) dissolving in water confirm this relation.

If the results with distilled water $\left(\mathscr{D}_{19\,^\circ\mathrm{C}} = 1.6 \times 10^{-5}\,\mathrm{cm}^2\,\mathrm{s}^{-1}\right)$ are taken as a basis, then the assumption of $\beta \propto \sqrt{\mathscr{D}}$ may be used to predict the values of mass transfer coefficients for bubbles of CO_2 rising in ethyl alcohol $\left(\mathscr{D}_{17\,^\circ\mathrm{C}} = 2.7 \times 10^{-5}\,\mathrm{cm}^2\,\mathrm{s}^{-1}\right)$. As may be seen from Figure 5, the experimental results are similar to the calculated results for bubbles of 0.8 cm to 1.0 cm equivalent radius. At larger radii the experimental results increase above the predicted values.

A. ALTERNATIVE EVALUATION OF Figure 2

If Figure 2 is redrawn (see Figure 8) and subjected to regression analysis, the following relationship will be obtained with a coefficient of determination 0f 0.963:

$$U = 22.374 \cdot R_c^{0.401} .$$

This may be approximated by the relation

$$U = 22.4 \cdot R_c^{\frac{2}{5}} .$$

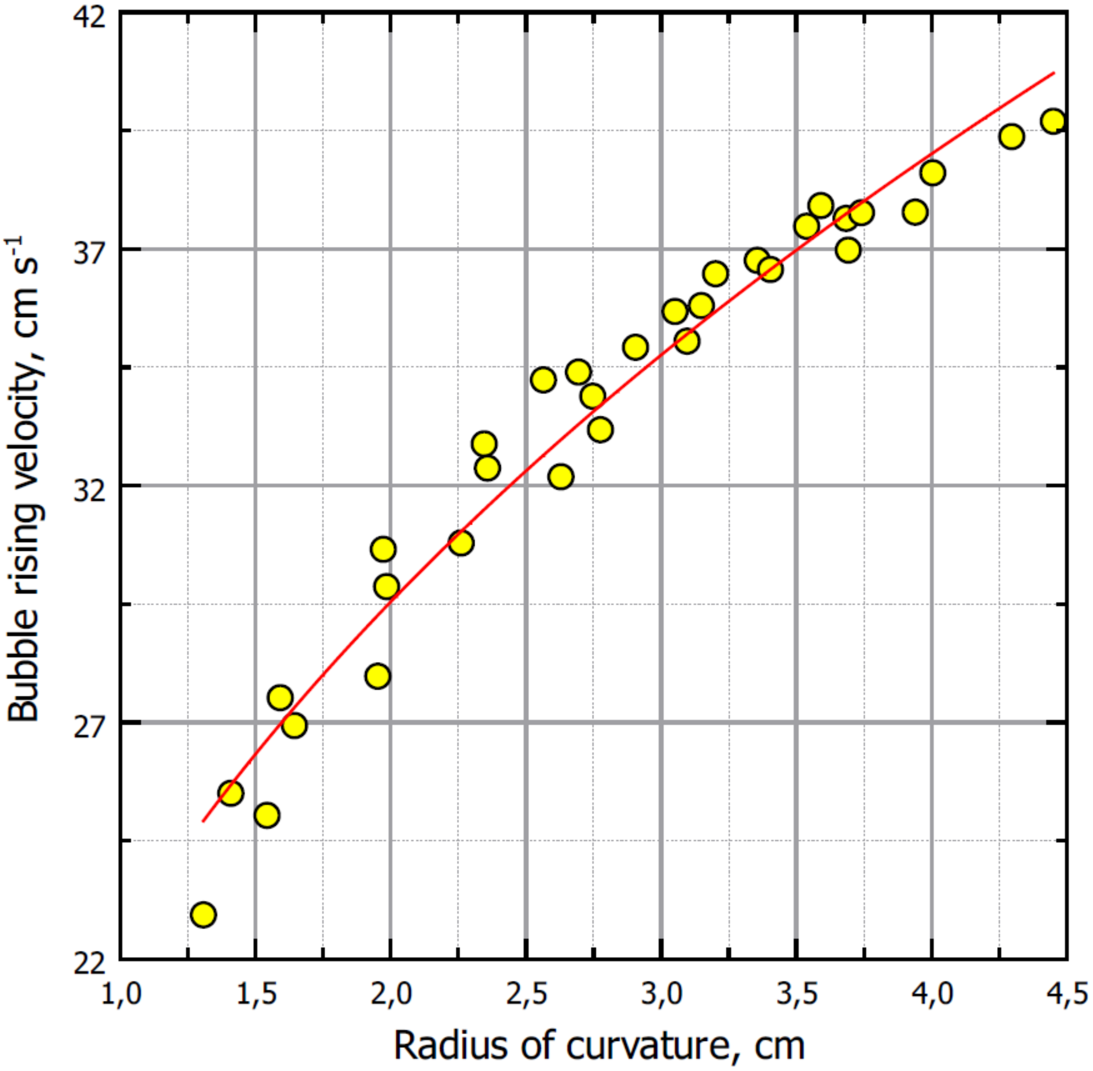

Figure 8: Rising velocity of bubbles in water plotted against radius of curvature

LIST OF SYMBOLS

A	surface area of a sphere of the same volume as the bubble
a	basal radius of the bubble
b	height of bubble
C	concentration of CO_2
C_d	coefficient of drag
$\mathscr{D}$	diffusion coefficient of CO_2 in appropriate solution
d_e	diameter of sphere of equivalent volume to bubble
d_c	diameter of column
E	width to height ratio of spherical cap bubble, $\frac{2a}{b}$
F_d	drag force
Fr	Froude number, $\frac{\rho_l U^2}{(\rho_l - \rho_g) \cdot g d_e}$
g	acceleration due to gravity
H	Henry's Law constant
K	coefficient
l	length of skirt from base of bubble
Mo	Morton number, $\frac{g \mu^4}{\rho_l \gamma^3}$
n	moles of CO_2 in bubble
$\dot{n}$	moles of CO_2 transferred to the bubble per unit time
P	pressure
$\mathscr{R}$	gas constant
R_c	radius of curvature
$\mathfrak{R}$	Reynolds number, $\frac{\rho_l U d_e}{\mu}$
r_e	equivalent radius (i.e. radius of sphere of equivalent volume to bubble)
S	shape factor, $(36\pi)^{\frac{1}{3}}$
t	time
U	terminal velocity of bubble in an infinite medium
$\overline{U}$	mean rising velocity of bubble
U_s	velocity of liquid at the gas-liquid interface relative to the bubble
U_w	velocity of a bubble influenced by proximity of column walls
V	volume of bubble
We	Weber number, $\frac{\rho_l U^2 d_e}{\gamma}$

y	distance along outward normal from bubble or skirt surface
z	vertical co-ordinate

α	half-angle subtended by bubble at centre of curvature
β	mass transfer coefficient
γ	surface tension
μ	dynamic viscosity of liquid
ρ	density
θ	temperature

$_b$	bulk of solution
$_B$	bubble
$_g$	gas
$_i$	interface
$_{hs}$	hydrostatic
$_l$	liquid

^{0}	at release
^{T}	at top of column

References

[1] H. Angelino. Hydrodynamique des grosses bulles dans les liquides visqueux. *Chemical Engineering Science*, 21(6-7):541–550, 1966.

[2] M. H. I. Baird and J. F. Davidson. Gas absorption by large rising bubbles. *Chemical Engineering Science*, 17(2):87–93, 1962.

[3] P. H. Calderbank and A. C. Lochiel. Mass transfer coefficients, velocities and shapes of carbon dioxide bubbles in free rise through distilled water. *Chemical Engineering Science*, 19(7):485–503, 1964.

[4] P. D. Coppock and G. T. Meiklejohn. The behavior of gas bubbles in relation to mass transfer. *Transactions of the Institution of Chemical Engineers*, 29:75–86, 1951.

[5] E. J. Cullen and J. F. Davidson. The effect of surface active agents on the rate of absorption of carbon dioxide by water. *Chemical Engineering Science*, 6(2):49–56, 1956.

[6] W. G. Davenport. *Bubbles in liquids including liquid metals.* PhD thesis, University of London, 1964.

[7] J. F. Davidson. Private communication.

[8] J. F. Davidson and E. J. Cullen. The determination of diffusion coefficients for sparingly soluble gases in liquids. *Transactions of the Institute of Chemical Engineers*, 35:51–60, 1957.

[9] J. F. Davidson and D. Harrison. *Fluidised Particles.* Cambridge University Press, New York, 1st edition, 1963. p. 134.

[10] R. M. Davies and G. I. Taylor. The mechanics of large bubbles rising through extended liquids and through liquids in tubes. *Transactions of the Royal Society of London. Series A, Mathematical and Physical Sciences*, 200(1062):375–390, 1950.

[11] W. L. Haberman and R. K. Morton. An experimental investigation of the drag and shape of air bubbles rising in various liquids. Technical Report 802, Navy Department, The David Taylor Model Basin, Washington 7, D.C., 1953. NS715-102.

[12] D. Hammerton and F. H. Garner. Gas Absorption from Single Bubbles. *Transactions of the Institution of Chemical Engineers*, 32:S18–S24, 1954.

[13] C. D. Hodgman. *Handbook of Chemistry and Physics.* Chemical Rubber Publishing Co., 41st edition, 1959.

[14] J. H. Leonard and G. Houghton. Mass transfer and velocity of rise phenomena for single bubbles. *Chemical Engineering Science*, 18(2):133–142, 1963.

[15] A. C. Lochiel and P. H. Calderbank. Mass transfer in the continuous phase around axisymmetric bodies of revolution. *Chemical Engineering Science*, 19(7):471–484, 1964.

[16] D. W. T. Rippin. *The Rise of Gas Bubbles in Liquids*. PhD thesis, University of Cambridge, 1959.

[17] A. Seidell. *Solubilities of Inorganic and Metal Organic Compounds*. D. Van Nostrand Co., Inc., New York City, 3rd edition, 1940.

[18] M. J. Stefan. Über die Diffusion der Kohlensäure durch Wasser und Alkohol. In *Sitzungsberichte der kaiserlichen Akademie der Wissenschaften, Mathematische-Naturwissenschaftliche Classe, II. Abtheilung*, volume 77, pages 371–409. K. K. Hof- und Staatsdruckerei in Commission bei Carl Gerold's Sohn, 1878.

[19] A. G. Szekely. Private communication.

[20] S. Uno and R. C. Kintner. Effect of wall proximity on the rate of rise of single air bubbles in a quiescent liquid. *American Institute of Chemical Engineers Journal*, 2(3):420–425, 1956.